Supplementary Information (SI) for Chemical Science.

Biological Semiconductors: Self-Assembled Shell Proteins as Photoactive Materials

Silky Bedi [a], S M Rose [a], Sharmistha Sinha*[a]

[a] Chemical Biology Unit, Institute of Nanoscience and Technology, Sector-81, Mohali, 140306

sinhas@inst.ac.in

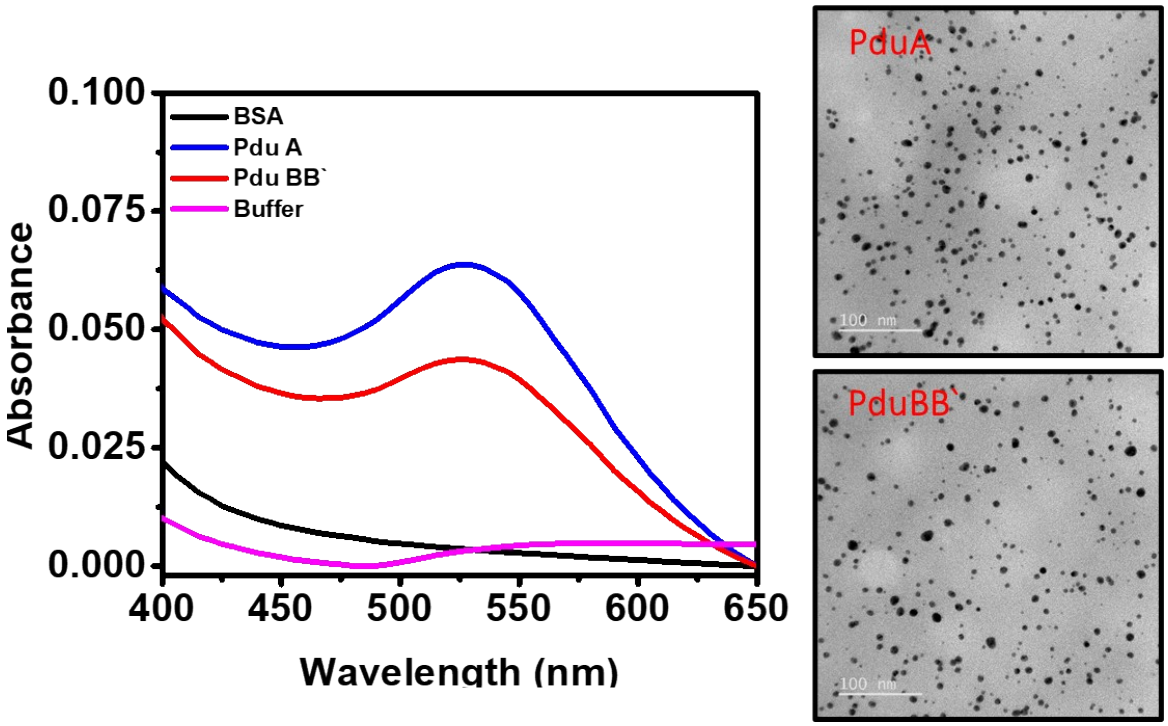

Figure S1. Synthesis and characterization of gold nanoparticles: Gold nanoparticles were synthesized using bacterial microcompartment shell proteins and conventional globular proteins as biotemplates. The formation of nanoparticles was initially confirmed by UV–visible absorption spectroscopy. TEM images further validate nanoparticle formation, revealing the morphology and distribution of gold nanoparticles

Protein Sequence of PduA:

MQQEALGMVETKGLTAAIEAADAMVKSANVMLVG**Y**EKIGSGLVTVIVRGDVGAVKAATDAGAAAAR
NVGEVKAVHVIPRPHTDVEKILPKGISQ

Protein Sequence of PduBB`:

MSSNELVEQIMAQVIARVATPEQQAIPGQPQPIRETAMAEKSCSLTEFVGTAIGDTLGLVIANVDTALLD
AMKLEKR**Y**RSIGILGARTGAGPHIMAADEAVKATNTEVVSIELPRDTKGGAGHGSLIILGGNDVSDVKRGI
EVALKELDRTFGDV**Y**GNEAGHIELQ**Y**TARAS**Y**ALEKAFGAPIGRACGIIVGAPASVGVLMADTALKSANV
EVVA**Y**SSPAHGTSFSNEAILVISGDSGAVRQAVTSAREIGKTVLATLGSEPKNDRPS**Y**I

Protein	No. of Tyrosine
PduA	1
PduBB’	6

Table S1: Protein sequences of PduA and PduBB` representing the number of tyrosine residues highlighted in red. PduA has one tyrosine residue instead PduBB` is having 6 residues per monomeric unit.

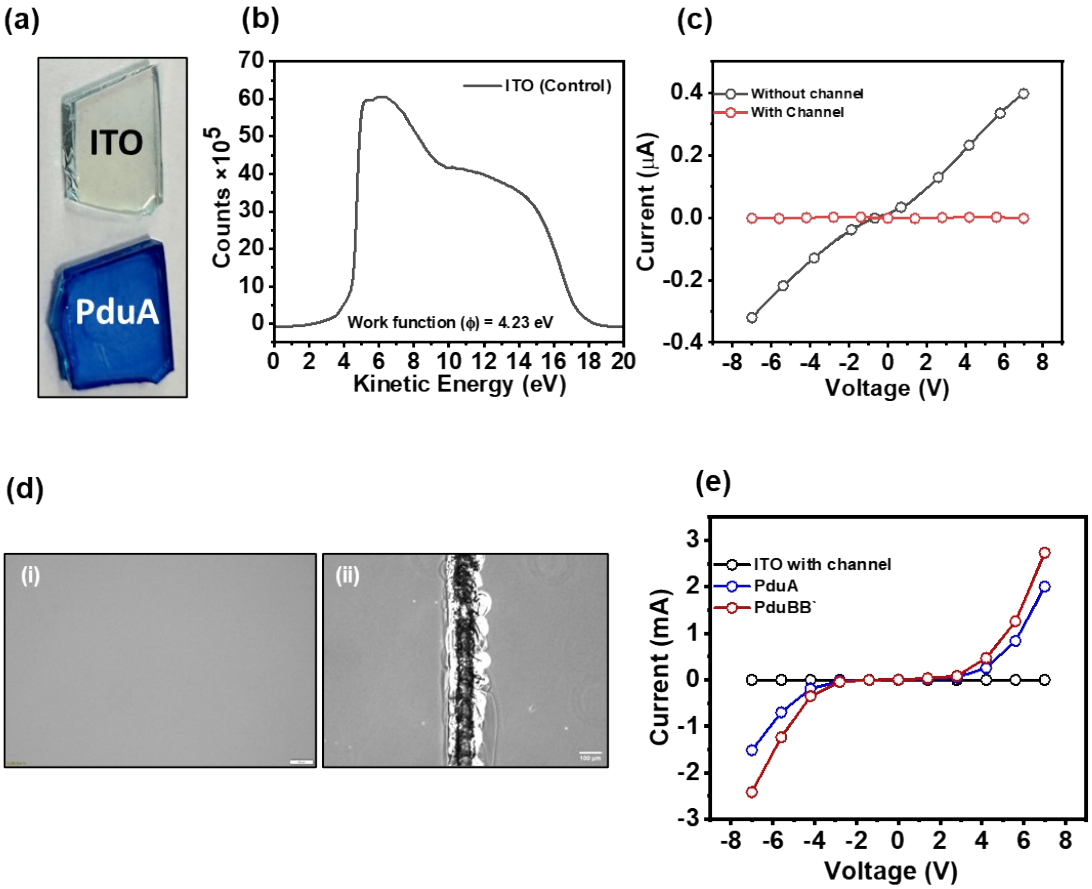

Figure S2: Electrical conductivity of control ITO substrate: (a) represents the bare ITO substrate and protein thick layer cast over the ITO substrate, stained with Coomassie Brilliant Blue R-250 dye to ensure protein coverage over the substrate; (b)Measured work function value of control ITO substrate; (c) I-V response of bare ITO without channel showing a linear increase in current on applying bias voltage corresponding to its conducting behavior and disruption in conductivity on casting channel on ITO substrate; (d) optical microscopic imaging of bare ITO substrate and casted channel over the ITO substrate surface, Scale bar- 100µM; (e) I-V response of ITO substrate with bare channel showing no electron conduction and in

presence of protein sample that bridges the connection between two ends of ITO substrate and show flow of current in a non-linear manner.

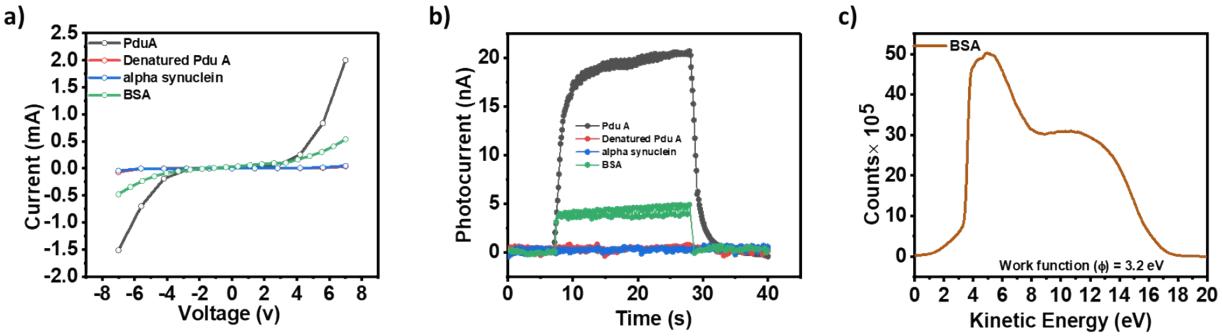

Figure S3: Electrical and photo responsive properties of different protein types: (a) I-V curves for shell protein PduA, heat denatured PduA, IDP-alpha synuclein and globular protein BSA demonstrating higher current flow for PduA compared to other; (b) Photocurrent responses of PduA , heat denatured PduA, IDP-alpha synuclein and globular protein BSA under UV light (254 nm) illumination, indicating that shell proteins exhibit significantly higher photo-responsivity than other. (c) Calculated work function (ϕ) values for BSA and shell proteins, with BSA showing a higher work function relative to shell proteins.

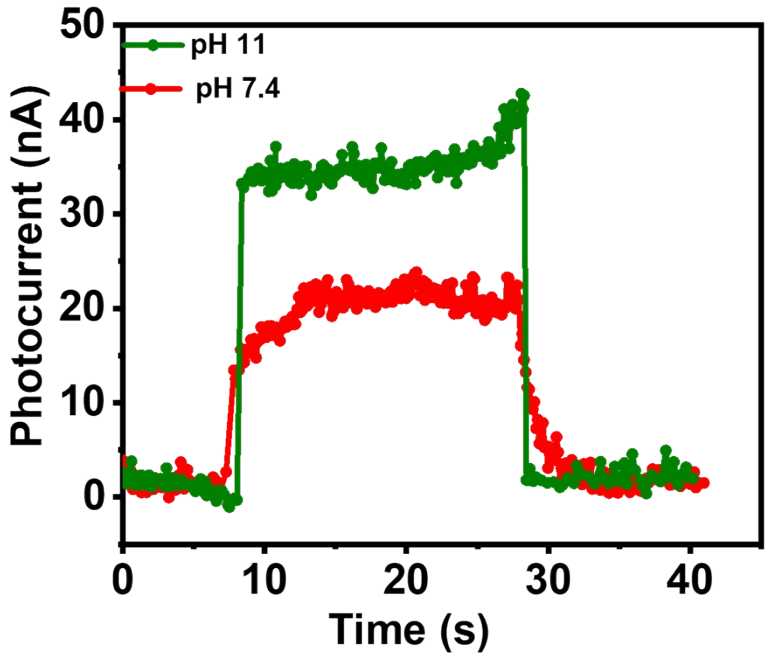

Figure S4: pH-dependent photocurrent response of PduA shell protein: Photocurrent measurements were performed using PduA shell protein under UV illumination at different pH conditions (pH 7.4 and 11.0) to probe the involvement of PCET mechanism. A notable increase in photocurrent was observed at pH 11.0, corresponding to the deprotonation of tyrosine residues (pKa ≈ 10.1). These results support the role of tyrosine-mediated electron transport in the intrinsic photoactivity of PduA.

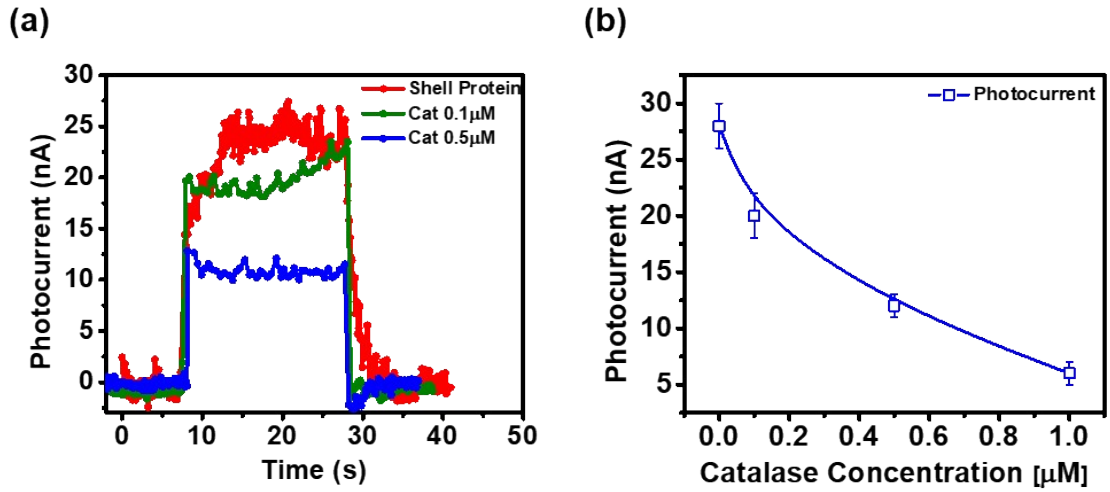

Figure S5: Effect of catalase on the photocurrent response of shell proteins: Photocurrent measurements were conducted in the presence and absence of catalase, a redox-active enzyme known to act as an electron scavenger in photoelectrochemical systems. A marked decrease in photocurrent upon catalase addition indicates that photogenerated electrons from the shell protein are being intercepted, supporting the involvement of a photo-induced electron transfer process.

	Primers used to generate mutant PduAY35A
Forward Primer (BglII)	gtgatgttagtgggcgccgaaaagattggc
Reverse Primer (HindIII)	gccaatcttttcggcgcccactaacatcac
Confirmed Sequence	**atg**caacaagaagcactaggaatggtagaaaccaaaggcttaaccgcagccatagaggccgctgatgcaatggttaagtcagccaatgtgatgttagtg gattggctccgggctggtaaccgtcatcgtgcgcggcgatgttggcgcggtcaaagcggccaccgatgcaggtgccgcagccgcacgcaacgtgggtgaa acacgtcatcccacgccctcacaccgatgtagaaaaaatcttaccgaagggaattagcca**atga**

Table S2: Forward and reverse primes create a point mutation in PduAWT to mutate tyrosine present at 35th position to alanine, generating a PduAY35A mutant. Point mutation is confirmed by doing the Sanger sequencing of the cloned plasmid having the gene of interest.

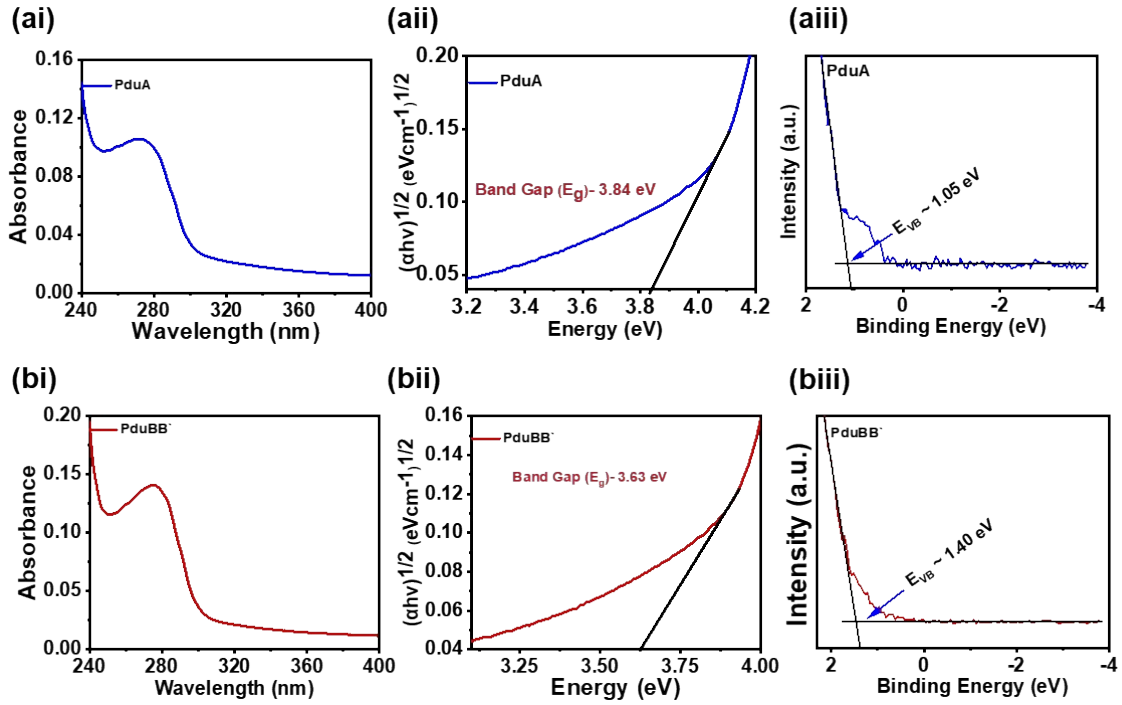

Figure S6: Band gap calculation for shell protein sheets: (ai) Absorbance spectrum of PduA (aii) Tauc plot derived from the absorbance spectrum to calculate the band gap for PduA shell protein; (aiii) Valence band calculation by extrapolating the UPS spectrum of PduA protein; (b i-iii) Absorbance spectrum, Tauc plot and extrapolated UPS spectrum for PduBB` shell protein.

	Primers used to generate mutant PduAY35W
Forward Primer (BglII)	5'-gcagcaagatctatgcatcaccatcatcaccaccaacaagaagcacta-3'
Reverse Primer (HindIII)	5'-gcctgcaagctttcattggctaattcc-3'
Confirmed Sequence	**atg**caacaagaagcactaggaatggtagaaaccaaaggcttaaccgcagccatagaggccgctgatgcaatggttaagtcagccaatgtgatgttagtggg ccccagaaaagattggctccgggctggtaaccgtcatcgtgcgcggcgatgttggcgcggtcaaagcggccaccgatgcaggtgccgcagccgcacgcaacgt gggtgaagtgaaagccgtacacgtcatcccacgccctcacaccgatgtagaaaaaatcttaccgaagggaattagcca**atga**

Table S3: Forward and reverse primes used to create point mutation in PduAWT to mutate tyrosine present at 35th position to try, generating PduAY35W mutant. Point mutation is confirmed by doing the Sanger sequencing of the cloned plasmid having the gene of interest.